XXXII Canary Islands Winter School of Astrophysics

Galaxy clusters in the local Universe

Andrea Biviano
INAF-Osservatorio Astronomico di Trieste

andrea.biviano@inaf.it
https://adlibitum.oats.inaf.it/biviano/

Lecture 4:

Masses & mass profiles

Based on:

Binney & Tremaine (1987),
Chapters 4.1, 4.2, 4.3

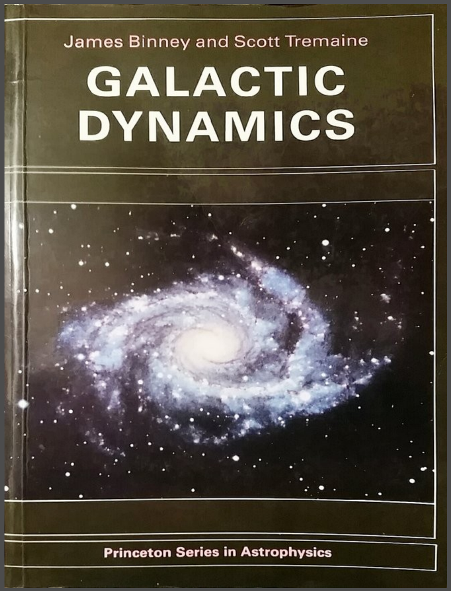

Pratt et al. (2019), Sections 2.3, 2.5, 3

Published: 28 February 2019

The Galaxy Cluster Mass Scale and Its Impact on Cosmological Constraints from the Cluster Population

G. W. Pratt, M. Arnaud, A. Biviano, D. Eckert, S. Ettori, D. Nagai, N. Okabe & T. H. Reiprich

Space Science Reviews **215**, Article number: 25 (2019) | Cite this article

Kneib (2008):

J.-P. Kneib: *Gravitational Lensing by Clusters of Galaxies*, Lect. Notes Phys. **740**, 213–253 (2008)
DOI 10.1007/978-1-4020-6941-3_7 © Springer Science+Business Media B.V. 2008

Additional readings:

Girardi et al. (1998), ApJ, 505, 74 *(on the virial theorem)*
Mamon, AB, Boué (2013), MNRAS, 429, 3079 *(the MAMPOSSt method)*

Masses & mass profiles

How can we estimate the masses and mass profiles of clusters of galaxies?

Masses & mass profiles

How we can estimate the masses and mass profiles of clusters of galaxies:

Gravitational lensing:

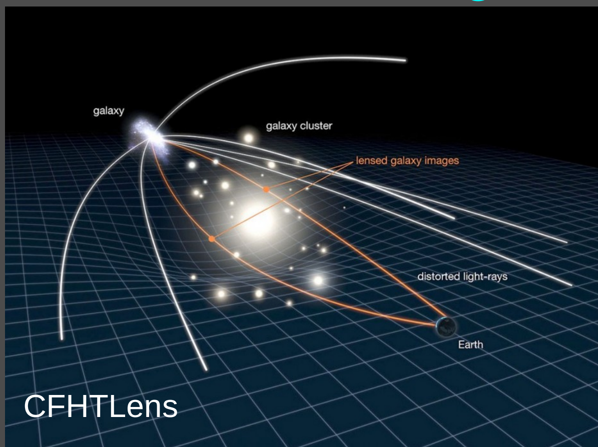

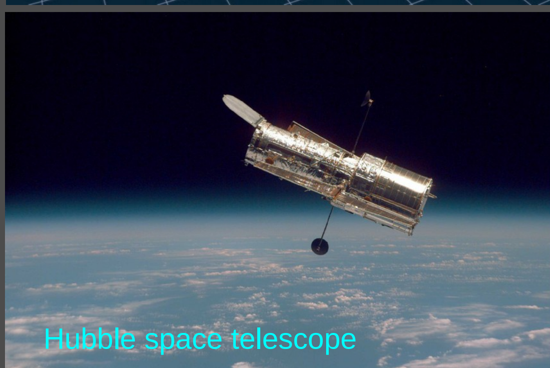

Optical-NIR observations: observing the effects of gravitational lensing by the cluster potential on the background galaxies

Intra-cluster plasma:

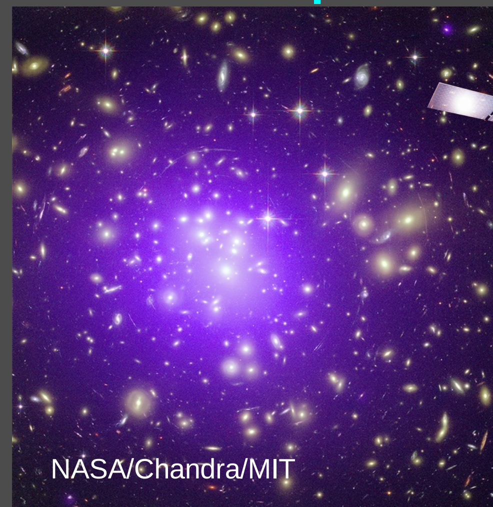

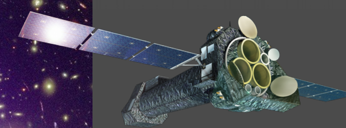

XMM-Newton space telescope

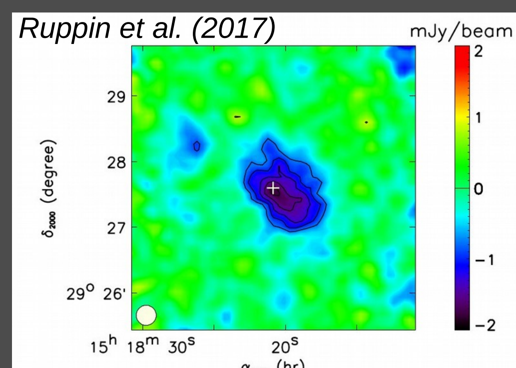

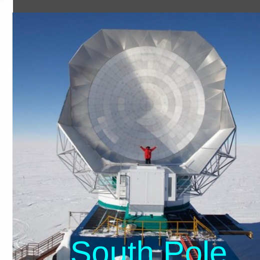

South Pole telescope

X-ray and radio (SZ) observations: assuming the intra-cluster, X-ray emitting gas is in hydrostatic equilibrium

Galaxies:

Optical-NIR observations: using the number, luminosity, and/or the spatial and velocity distributions of cluster galaxies

Masses & mass profiles

Gravitational lensing

Images of background galaxies are distorted by the cluster gravitational field;

if the alignment observer-cluster-source is good, the wave front is broken in multiple pieces by the grav. field and multiple images arise
⇒ **strong lensing**

if the alignment is less good, the distortion of the source is less important
⇒ **weak lensing**

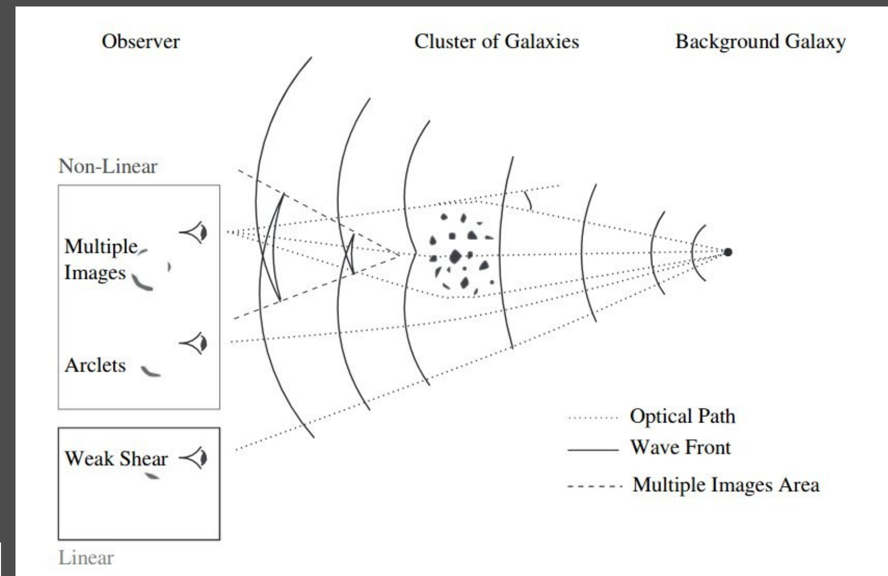

Basic equations:

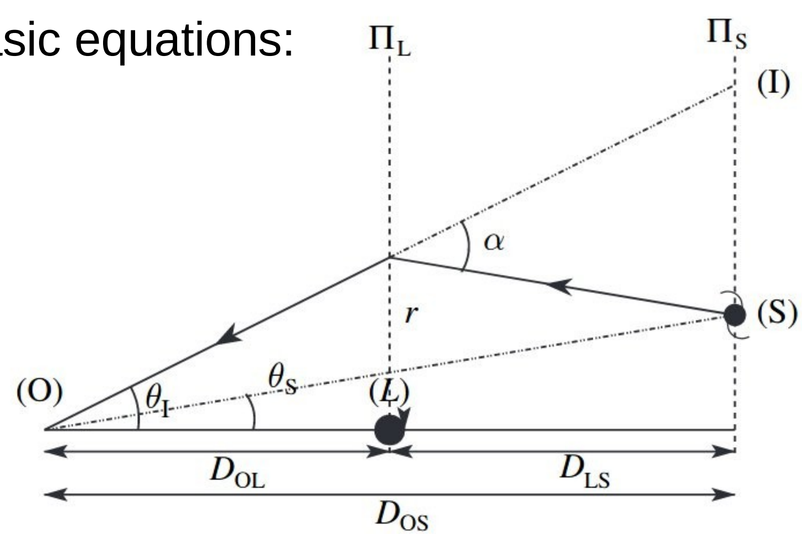

Kneib (2008)

$$\boldsymbol{\theta}_I = \boldsymbol{\theta}_S + \frac{D_{LS}}{D_{OS}}\boldsymbol{\alpha}$$

$\varepsilon = D_{LS}/D_{OS}$

$$\boldsymbol{\alpha}(\boldsymbol{\theta}_I) = \frac{2}{c^2}\frac{D_{LS}}{D_{OS}}\nabla_{\boldsymbol{\theta}_I}\phi_N^{2D}(\boldsymbol{\theta}_I)$$

Φ_N^{2D}= =projected potential

$$\boldsymbol{\theta}_S = \boldsymbol{\theta}_I - \frac{2\mathcal{E}}{c^2}\nabla\phi_N^{2D}(\boldsymbol{\theta}_I) = \boldsymbol{\theta}_I - \nabla\varphi(\boldsymbol{\theta}_I)$$

φ≡"lensing potential"

$$M(r) = \frac{c^2}{4G}\frac{D_{OS}D_{OL}}{D_{LS}}r\partial_r\varphi(r)$$

...in circular symmetry

Masses & mass profiles

Gravitational lensing

GL can allow a high level of accuracy and precision in the determination of cluster mass distribution. The best example is that of **SN "Refsdal"** observed behind a massive z=0.5 cluster

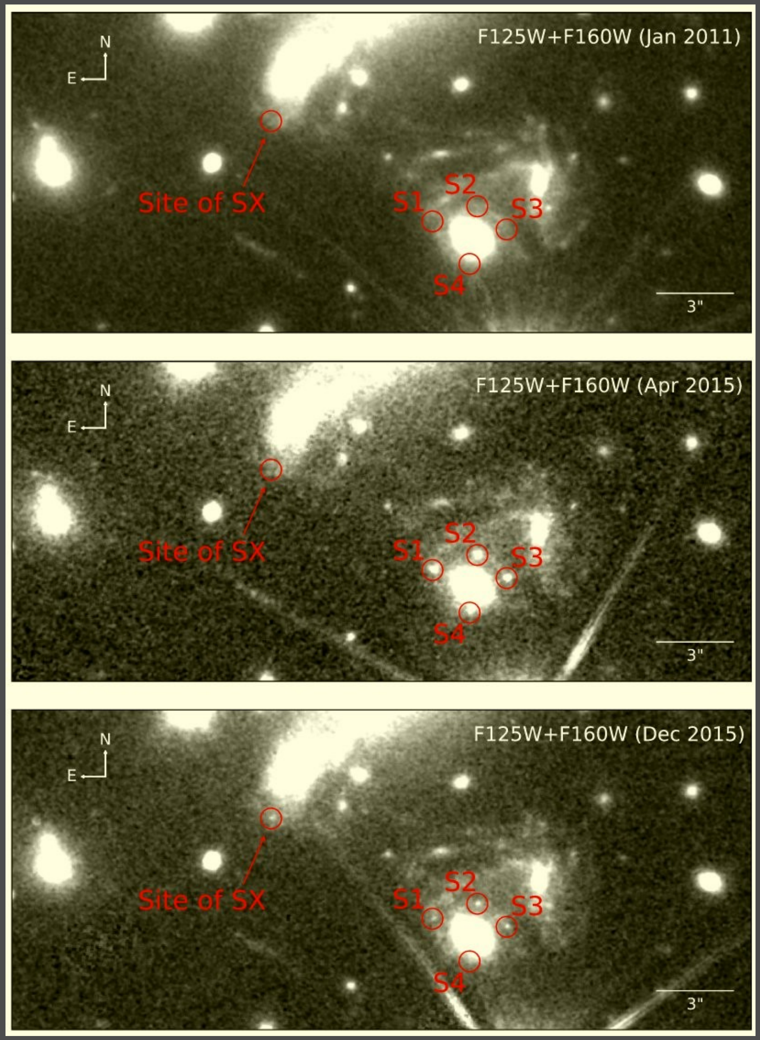

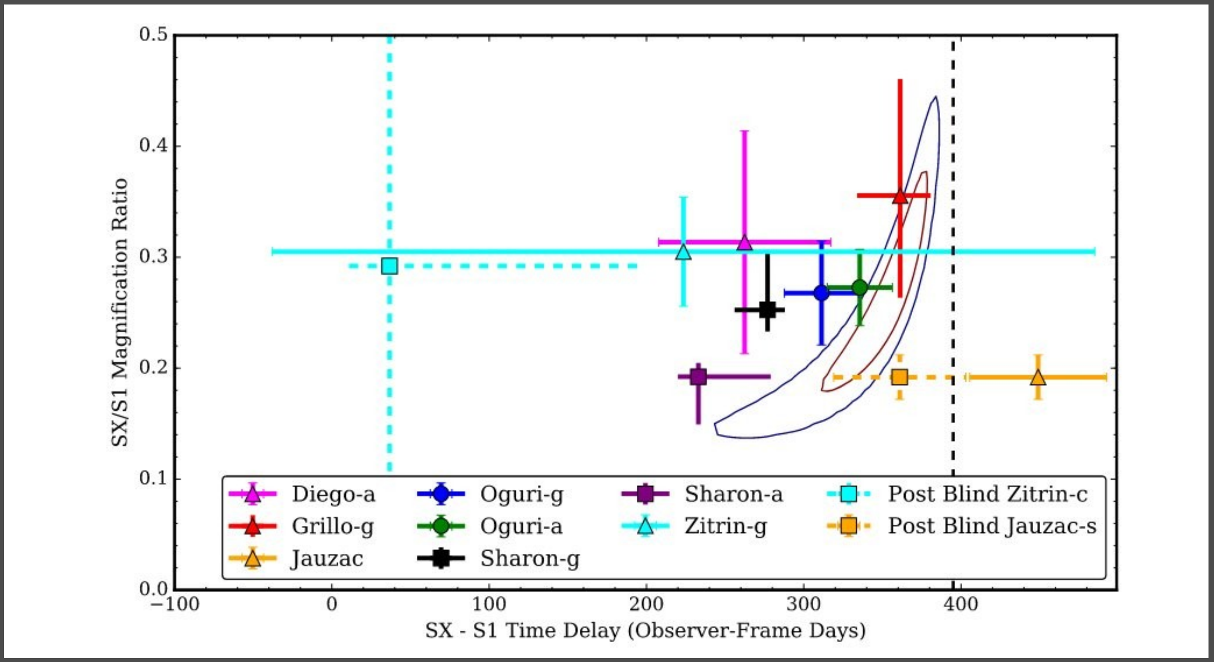

Kelly et al. (2016)

SN lensed image first appeared in Nov 2014; models for the projected mass distribution in the cluster were able to predict the time and location of the re-appearance of the same SN (the light of the SN coming to us through a different lensing path)

Masses & mass profiles

Gravitational lensing

However there are several sources of **systematic uncertainties**:

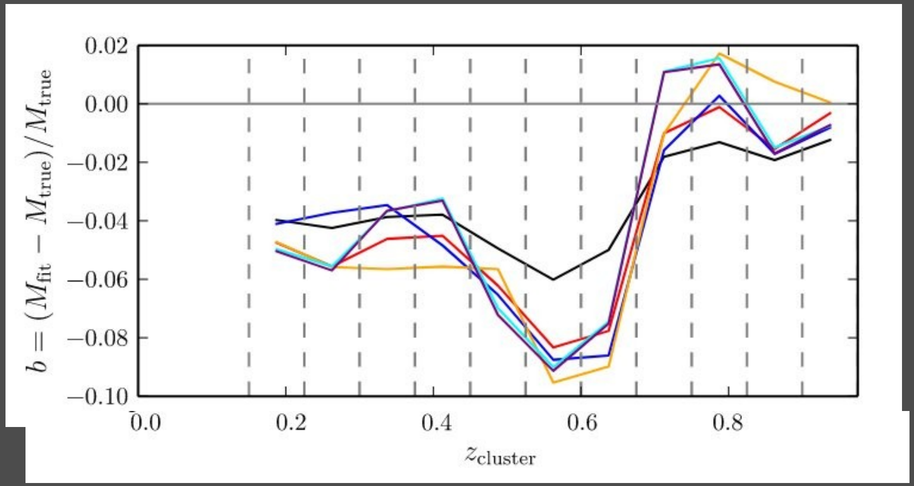

Contamination of the data set of background lensed galaxies by cluster members – they dilute the lensing signal. The effect depends on the galaxy type and redshift *(Kohlinger et al. 2015)*

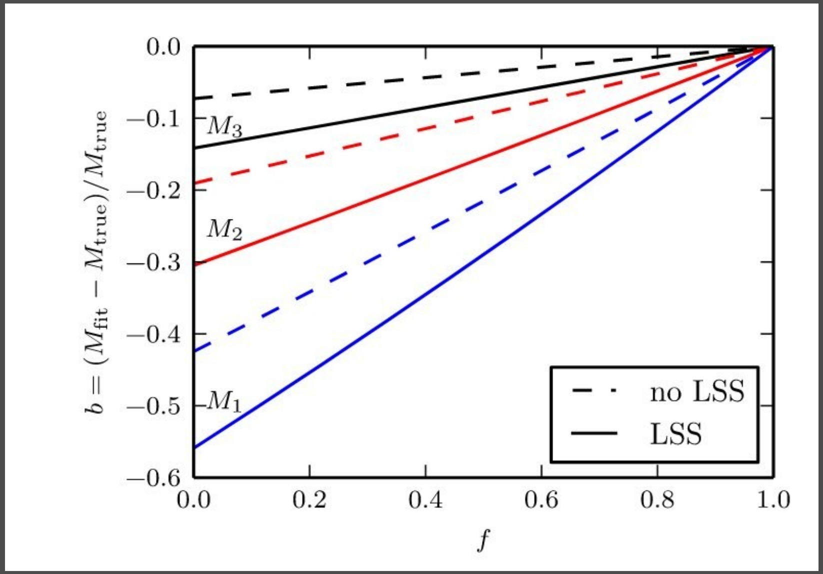

Mis-centering:
the mass bias for a stack sample of clusters depends on the fraction 1-f of mis-centered clusters *(Kohlinger et al. 2015)*

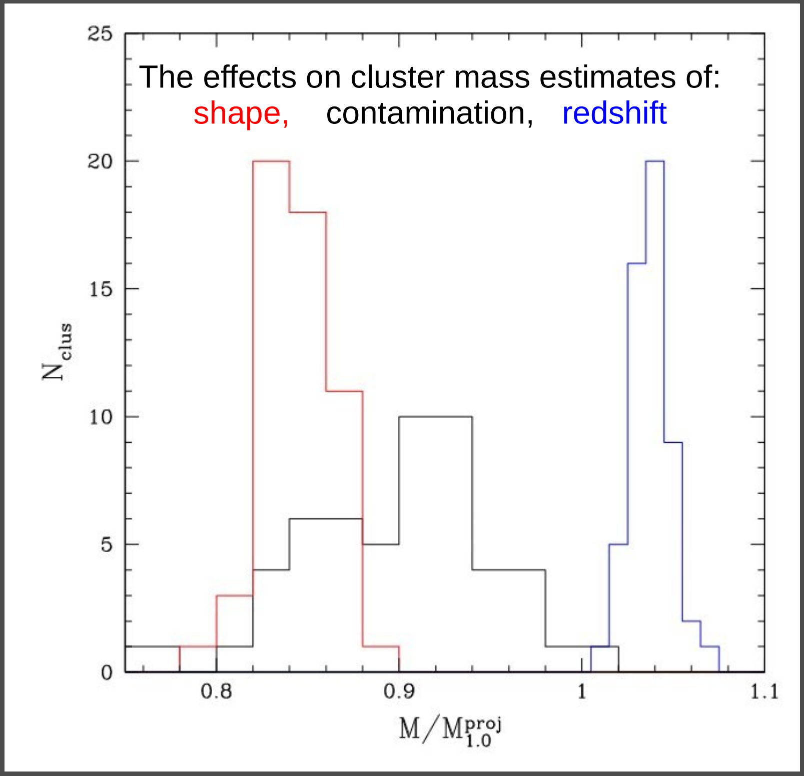

Shape measurement accuracy, **contamination**, incorrect **redshift distribution** of lensed galaxies *(Hoekstra et al. 2015)*

Masses & mass profiles

Gravitational lensing

These systematic uncertainties create **scatter** in the GL mass estimates:

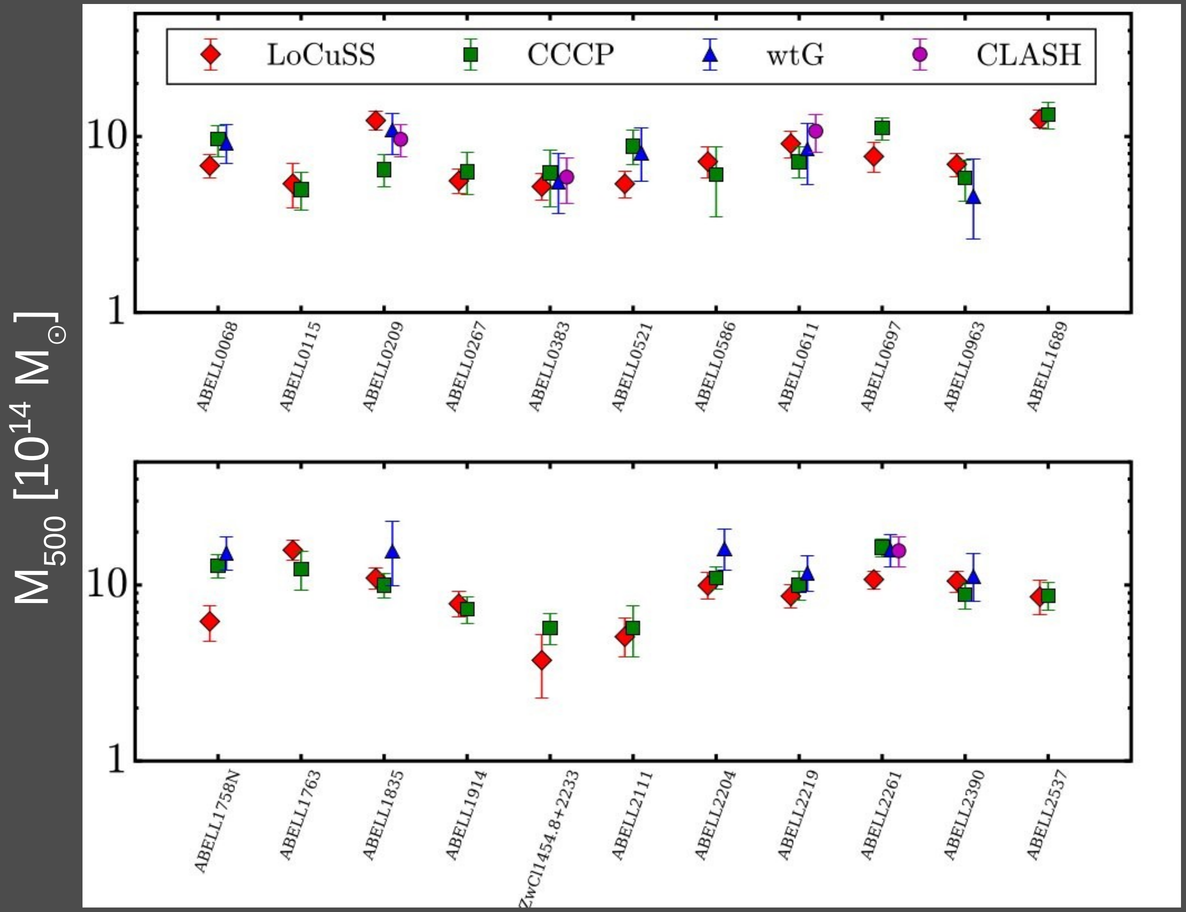

Pratt et al. (2019): comparison of different weak lensing mass determinations within a radius r_{500}

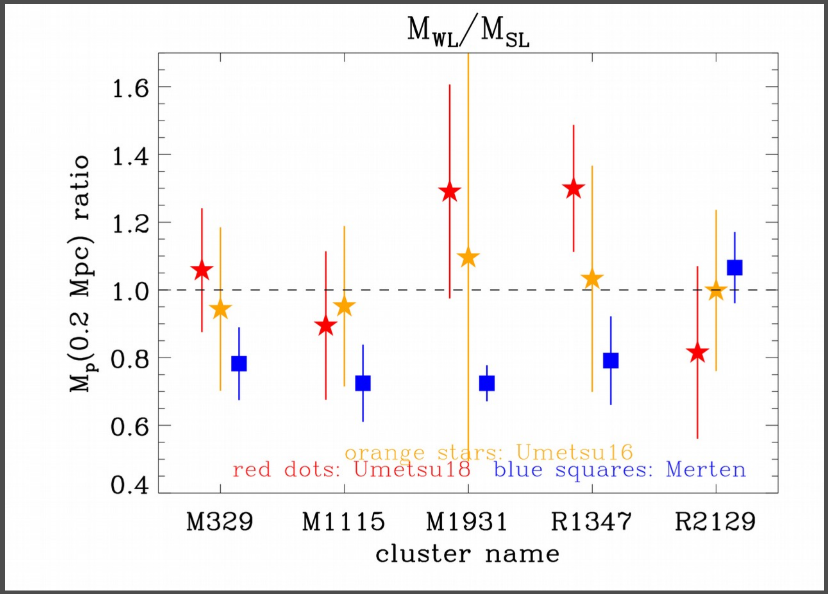

AB (unpublished): comparison of weak lensing to strong lensing masses within a radius of 0.2 Mpc

Masses & mass profiles

Gravitational lensing

Most important: GL measures the **projected** mass

We see a massive cluster in projection... but what we measure is its mass + the mass of hidden structures behind (or in front), if they are not well separated in (photometric) redshift

Even if the cluster does not hide other structures along the line-of-sight, it is generally not spherical, so the measured mass is a function of the relative orientation of the cluster main axis and the line-of-sight *(Osato et al. 2018).*

Since a cluster is more likely to give a strong GL signal if it is elongated along the line-of-sight this creates an "orientation bias" in the selection of clusters as strong lenses.

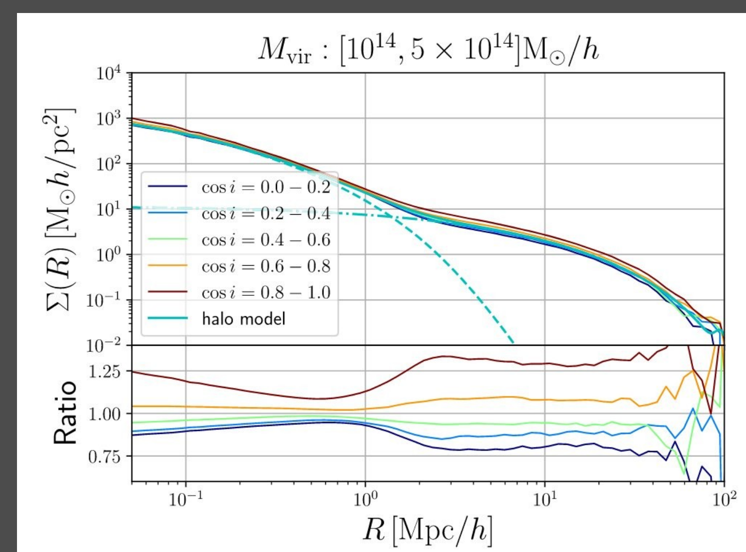

Masses & mass profiles

Intra-cluster plasma

The deep potential well of clusters compresses the collapsing gas heating it to $T \geq 10^7$ K, the intra-cluster (IC) plasma emits (mostly) via thermal **Bremsstrahlung** in X-rays, $\epsilon \propto \rho_{gas} T^{1/2}$.

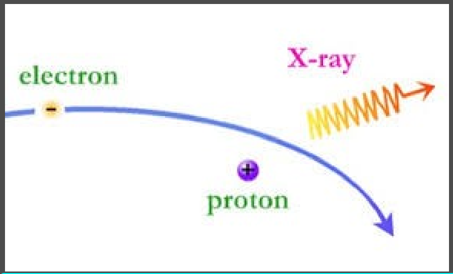

Inverse Compton scattering of CMB photons by the IC plasma electrons produces the SZ effect *(Sunyaev & Zeldovich 1972)* observed at radio (mm) wavelengths.

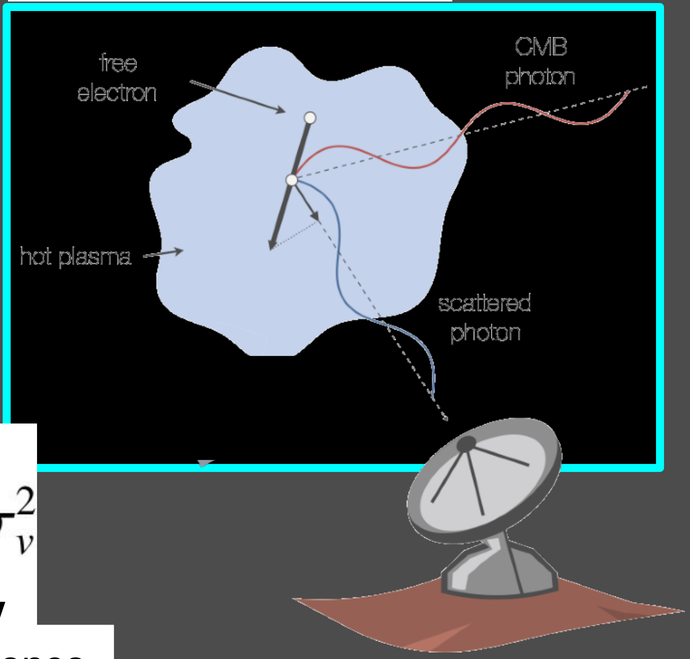

Basic equations:

(Euler)

$$\frac{\partial \mathbf{v}}{\partial t} + (\mathbf{v} \cdot \nabla)\,\mathbf{v} + \frac{1}{\rho_{gas}} \nabla P_{gas} = -\nabla \Phi$$

After thermalization of the kinetic energy the velocity field becomes negligible

$$M_{tot}(< r) = -\frac{r\, P_{gas}}{\mu m_u G\, n_{gas}} \frac{d \log P_{gas}}{d \log r}$$

(Hydrostatic Equilibrium)

$$P_{tot} \simeq P_{gas} + \frac{1}{3} \rho\, \sigma_v^2$$

turbulence

SZ

$$y = \frac{\sigma_T}{m_e c^2} \int P_{tot}\, dl \qquad \frac{\Delta I_{tSZ}}{I_0} = y f(\nu, T_e)$$

$P_{gas} = k\, \rho_{gas} T$, with:

ρ_{gas} from deprojection of X-ray surface brightness

T from X-ray spectra extracted in annuli

or P_{tot} directly from SZ

Masses & mass profiles

Intra-cluster plasma

When P_{gas} cannot be determined as a function of radius (for lack of photons or angular resolution) it is still possible to use **proxies** for the cluster mass *(not for the mass profile, however)*, modulo the redshift dependence parametrized by $E(z)^2 \equiv \Omega_0 (1+z)^3 + \Omega_\Lambda + \Omega_R (1+z)^2$

- from mm observations: the integrated SZ signal $Y_{SZ} \equiv \int y \, d\Omega$
- from X-ray observations:
  the X-ray luminosity L_X, the mean plasma temperature T, the total gas mass M_{gas}, and their combination $Y_X \equiv T \, M_{gas}$ *(Kravtsov et al. 2006)*

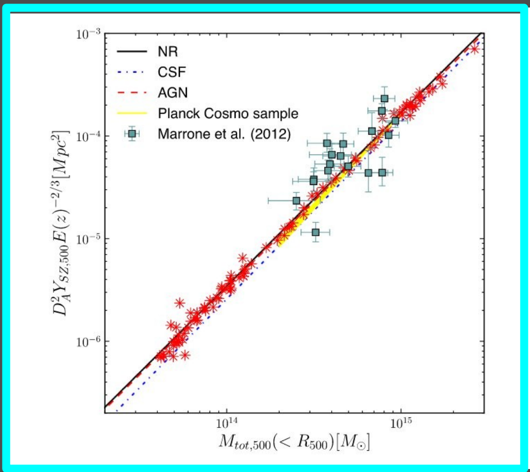

Planelles et al. (2017)

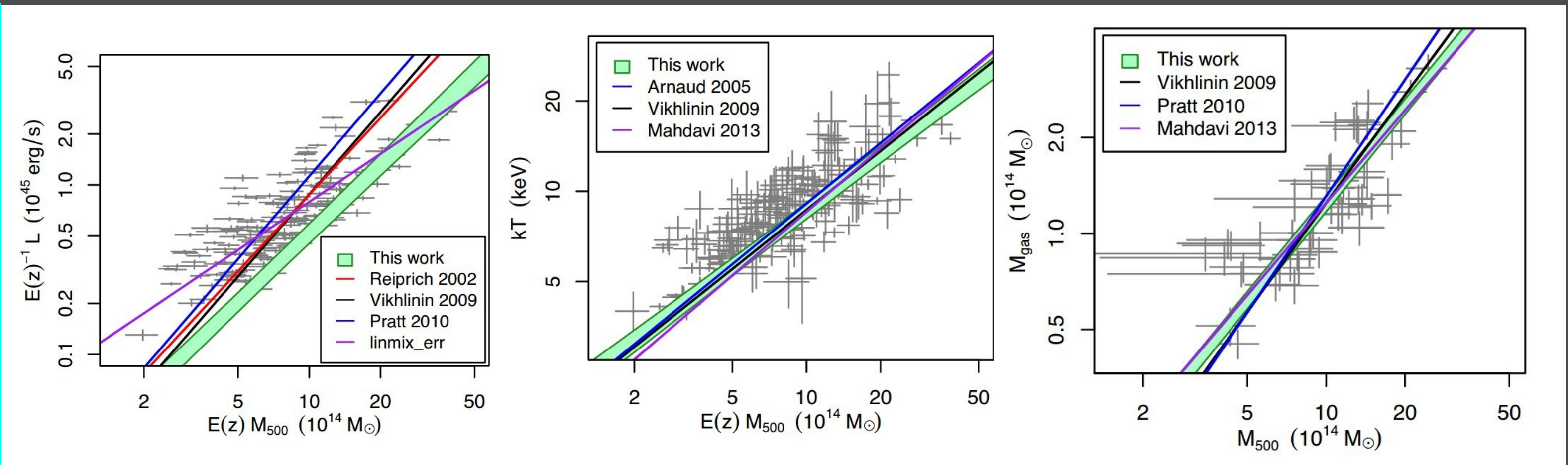

Mantz et al. (2016)

Masses & mass profiles

Intra-cluster plasma

Machine Learning approach may prove superior to traditional ones, and estimate the cluster mass directly from (e.g.) the SZ image or from a combination of several mass proxies

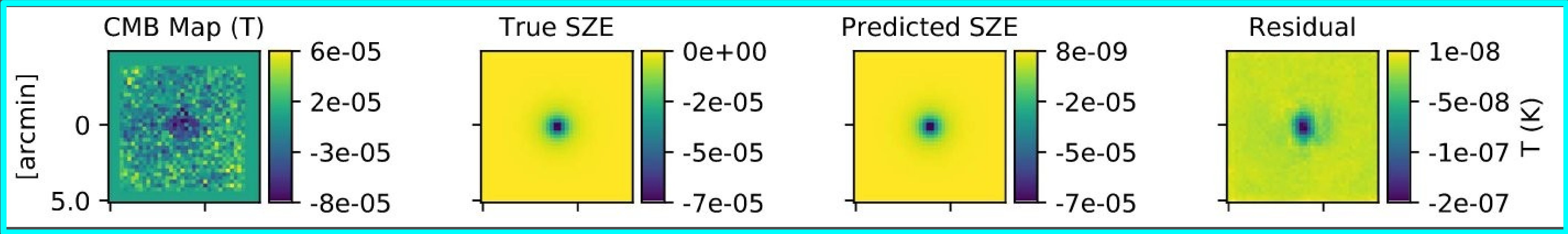

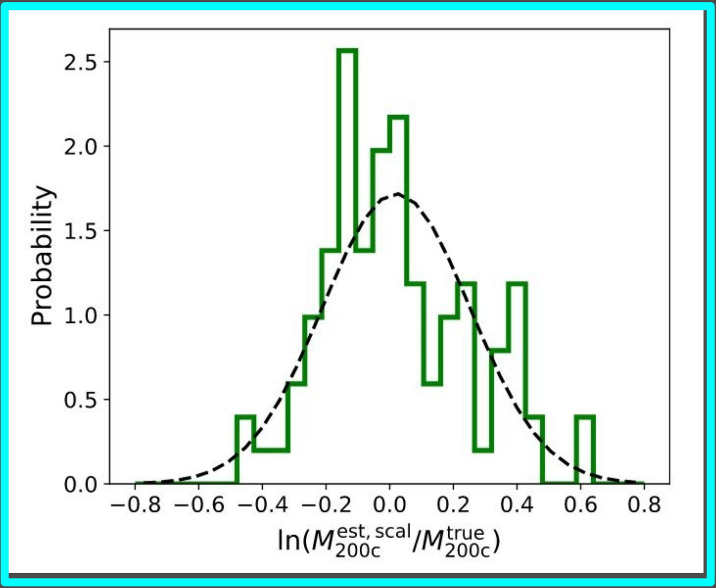

Gupta & Reichardt (2020):
use SZ images

Yan et al. (2020):
consider several mass tracers, including stellar mass, X-ray fluxes, SZ

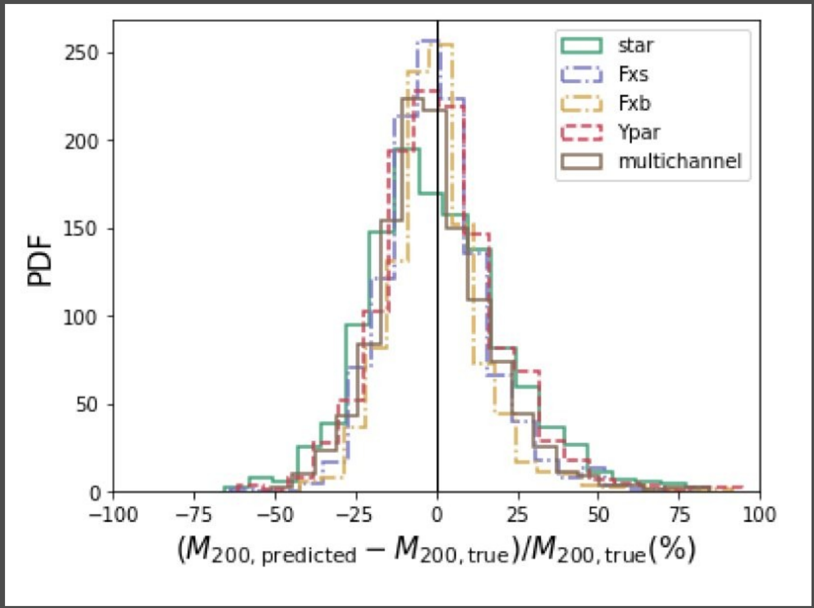

Masses & mass profiles

Intra-cluster plasma

Systematic uncertainties for the intra-cluster plasma-based mass estimates

1. Hydrostatic mass bias: $$P_{\rm tot} \simeq P_{\rm th} + \frac{1}{3}\rho\sigma_v^2 \longrightarrow P_{NT}$$

Non-thermal pressure P_{NT} can be estimated by: *a)* comparing the measured baryon fraction in clusters (mostly contributed by the intra-cluster plasma) to the Universal value of baryon fraction (CMB studies), *b)* by combining X-ray, SZ, and GL estimates, *c)* via numerical simulations

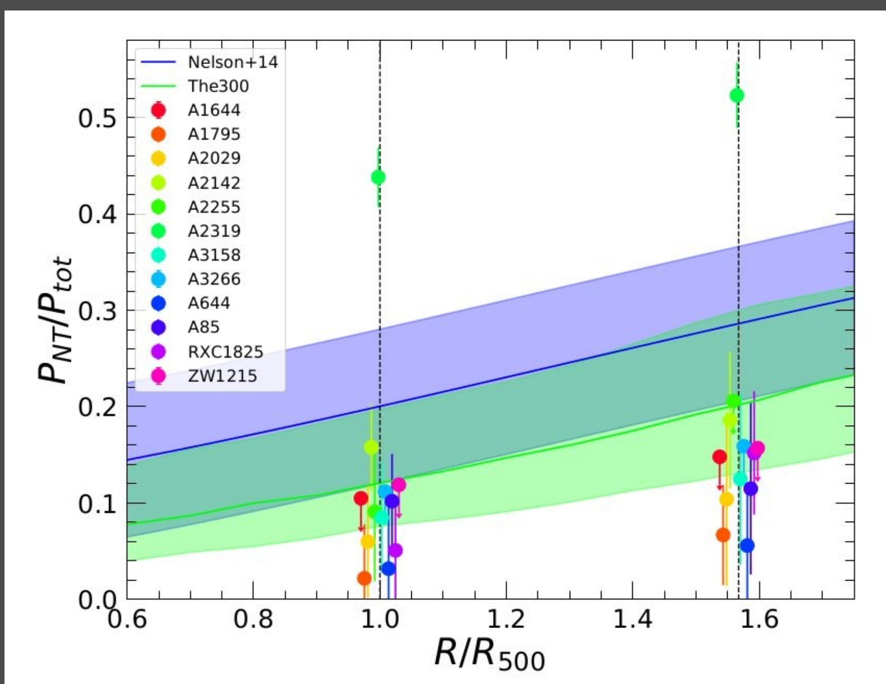

Pratt et al. (2019): using baryon fraction

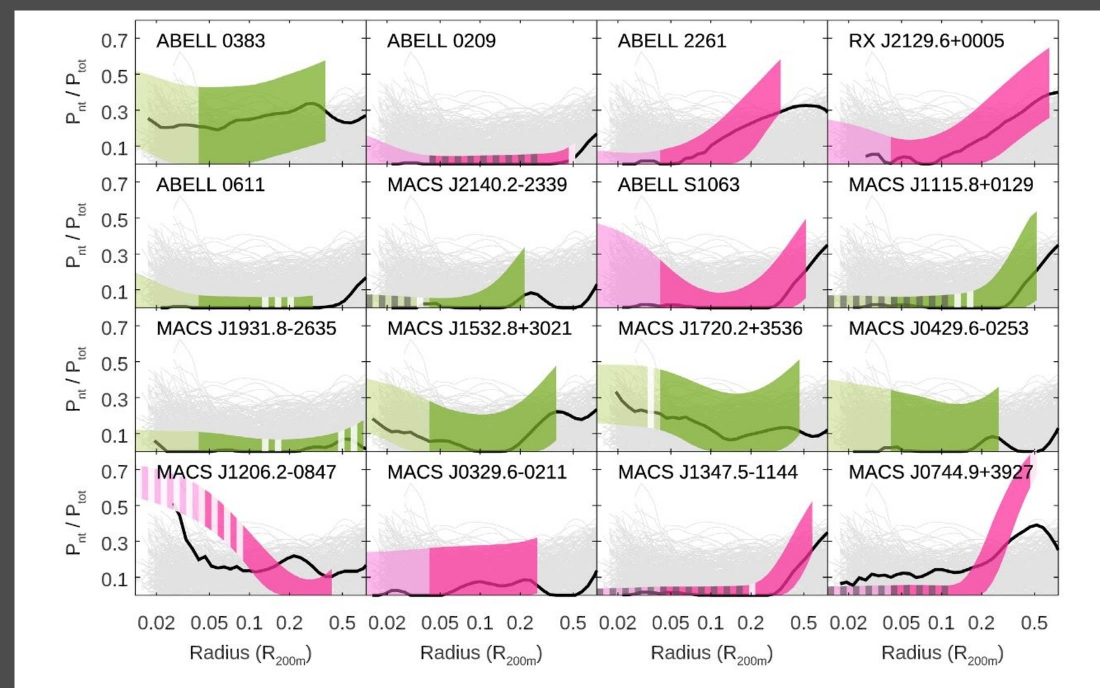

Sayers et al. (2021): using GL, X-ray and SZ (green: relaxed clusters, magenta: mergers; grey: simulations)

Masses & mass profiles

Intra-cluster plasma

Incomplete thermalization can also be identified directly by the measurement of **bulk flows**. *Hitomi collaboration (2016)* measured a velocity width of ~150 km/s in the emission lines of the intra-cluster plasma at the center of the Perseus cluster, corresponding to P_{NT}/P_{tot}~4%

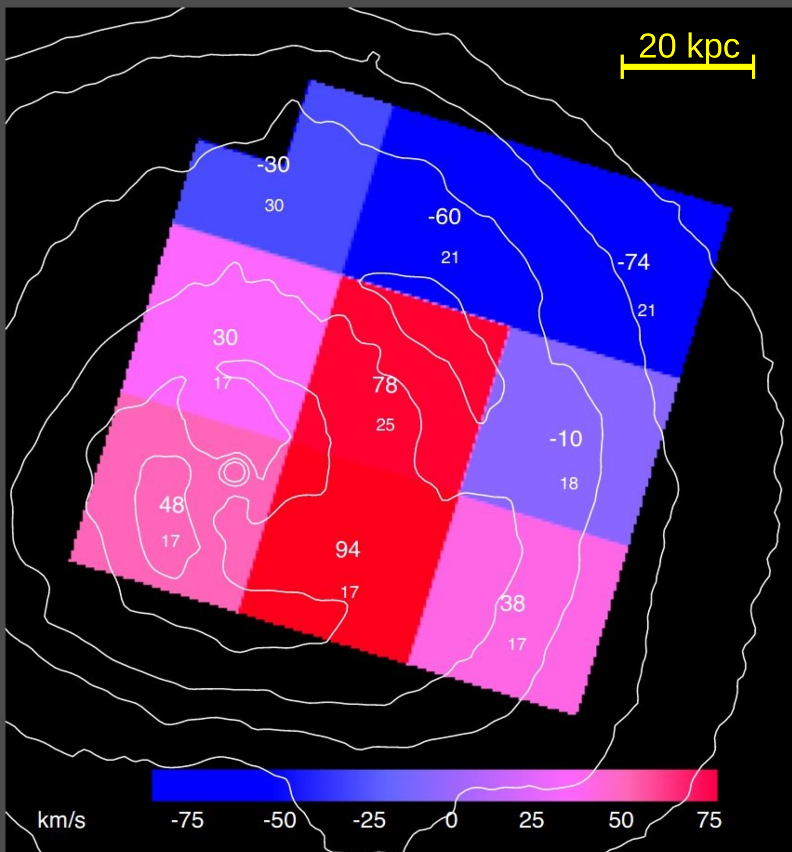

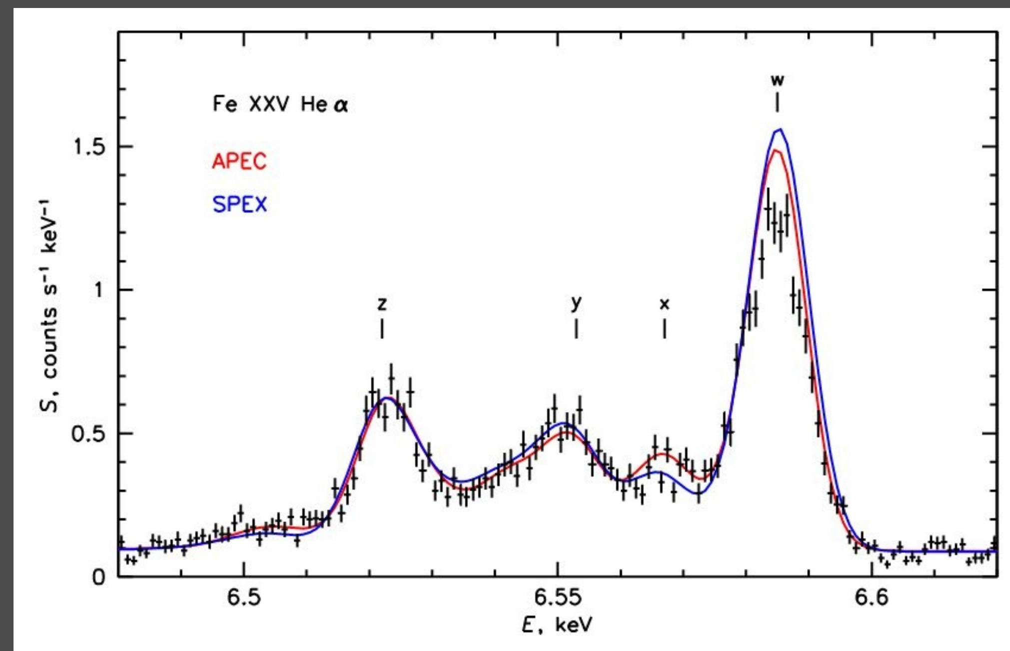

Less precise measurements with Chandra *(Liu et al. 2016)* and Suzaku *(Ota & Yoshida 2016)* do however indicate intra-cluster plasma bulk flows >1000 km/s in some clusters

Masses & mass profiles

Intra-cluster plasma

Bulk motions in the intra-cluster plasma are probably generated by **cluster-subcluster collisions**.

Identifying substructures can help reducing systematics.

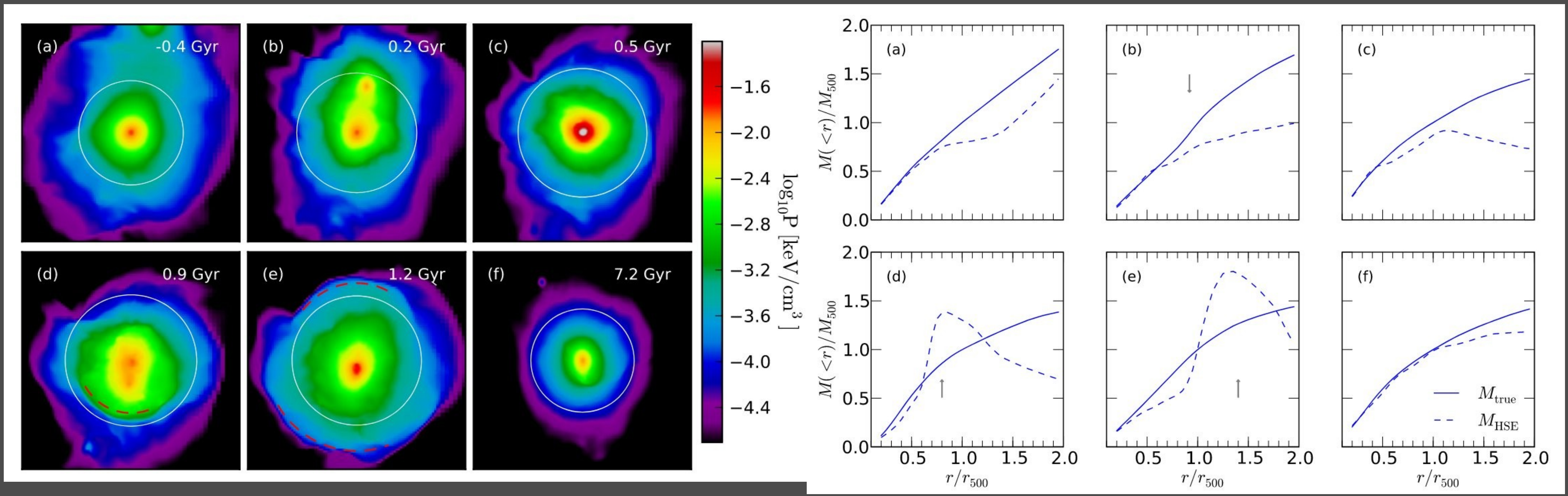

Nelson et al. (2012): a cluster merger from high-resolution cosmological simulations
(right-hand panel: solid/dashed lines = true mass/estimated mass)

Masses & mass profiles

Intra-cluster plasma

Other systematic uncertainties come from:

- plasma temperature **inhomogeneities**
- absolute X-ray temperature **calibration**

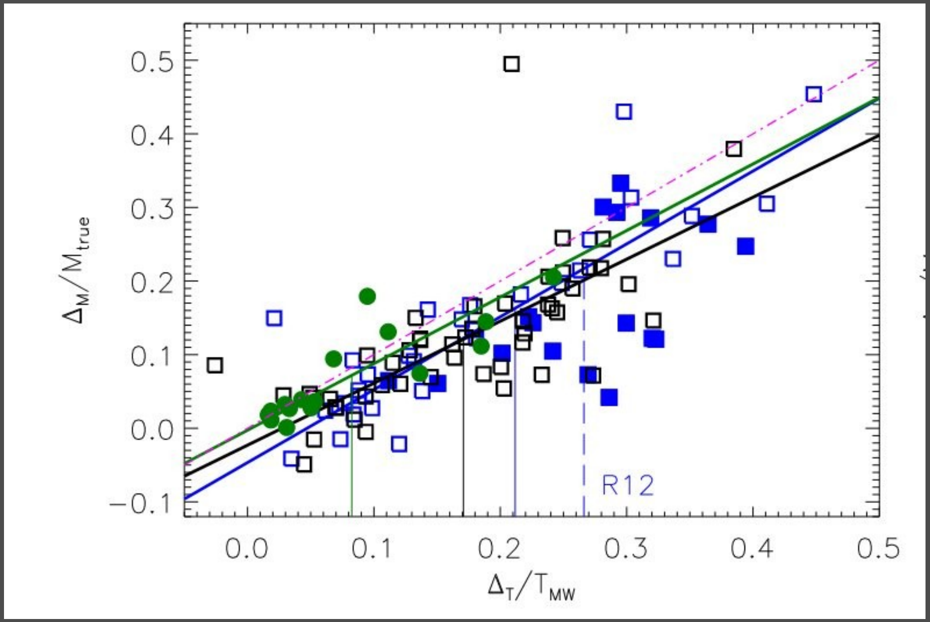

Numerical simulations of *Rasia et al. (2014)*: change in hydrostatic mass estimates due to temperature inhomogeneities that cause differences between the mass-weighted temperature and the measured spectroscopic one

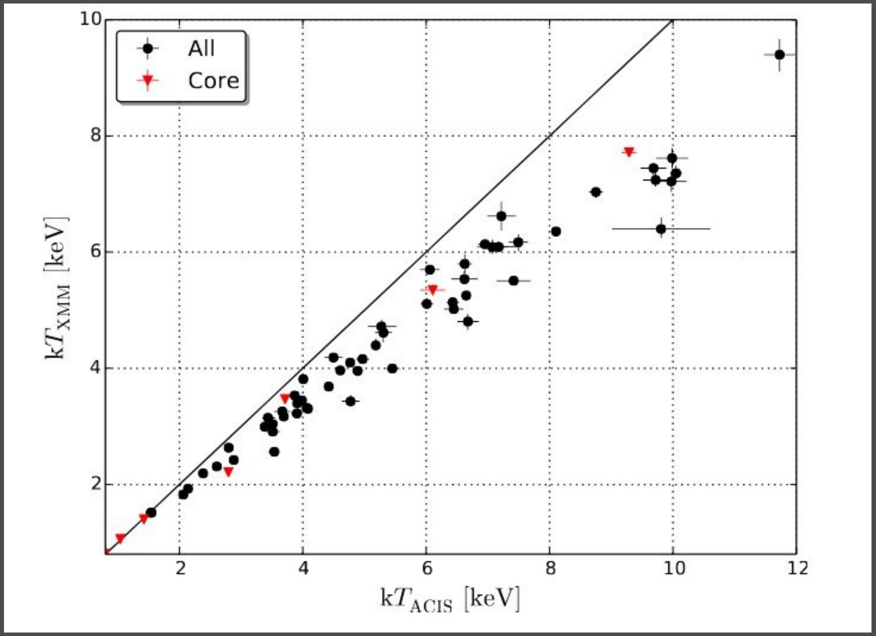

Schallenberger et al. (2015): temperatures measured with XMM and with Chandra for 64 clusters

Masses & mass profiles

Intra-cluster plasma

These systematic uncertainties create **scatter** in the X-ray mass estimates:

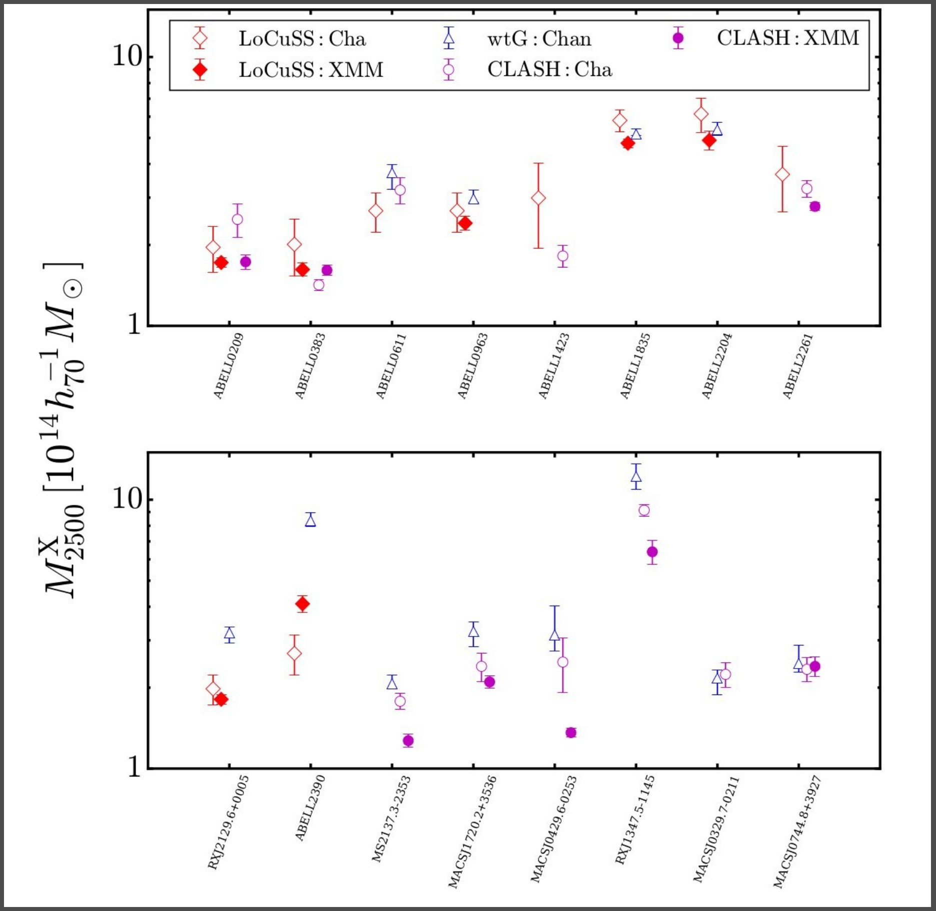

Pratt et al. (2019): comparison of X-ray mass determinations within a radius r_{2500}

These systematics also create **biases** in the X-ray mass estimates, but not strong enough to reconcile the number of massive clusters we observe with that expected in Planck CMB cosmology

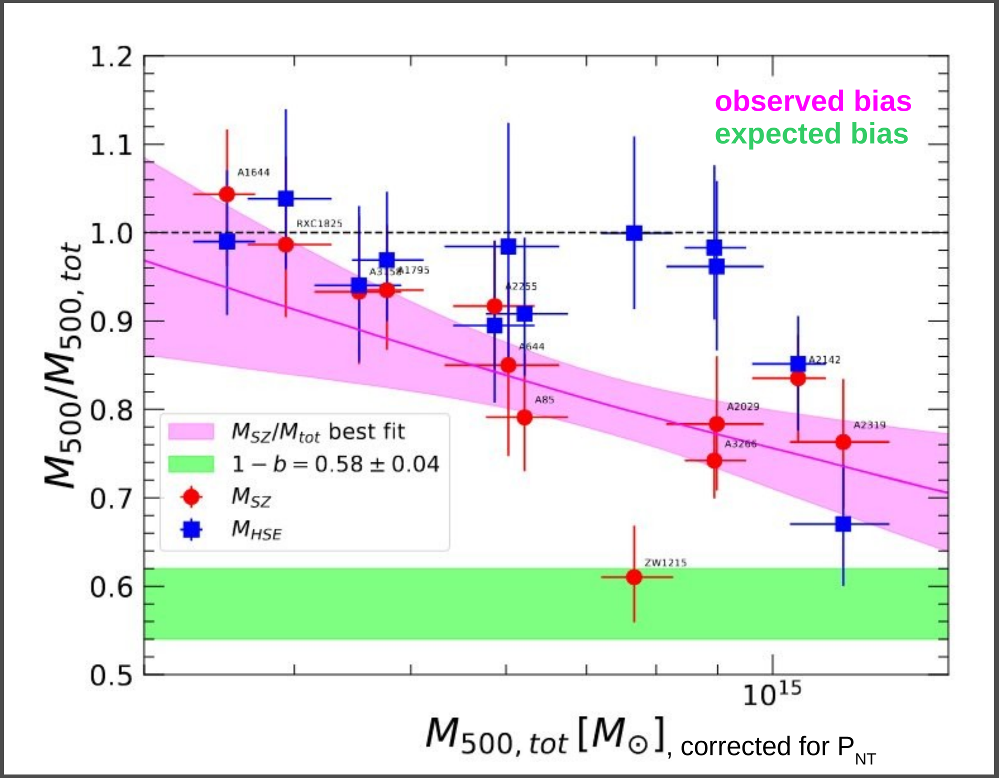

Eckert et al. (2019): observed bias in the X-ray mass estimates of 13 clusters (*magenta*) vs. expected bias needed to reconcile Planck SZ cluster counts with expected from Planck CMB cosmology (*green*)